Recognizing gender from images with facial makeup

Annie Micheal[1], Geetha Palanisamy[2]
[1]Department of Computer Science and Engineering, Sathyabama Institute of Science and Technology, Chennai, India
[2]Department of Information Science and Technology, College of Engineering Guindy, Anna University, Chennai, India

Article Info

Article history:

Received Jan 12, 2024
Revised Mar 16, 2024
Accepted Apr 13, 2024

Keywords:

Dense SIFT
DT-CWT
LS-SVM
Log-Gabor COSFIRE

ABSTRACT

Recognizing the sex of an individual is a difficult task due to pose variation, occlusion, illumination effect, facial expression, plastic surgery, and makeup. In this manuscript, a novel approach for gender recognition with facial makeup is proposed. A novel Log-Gabor COSFIRE (LG-COSFIRE) filter is a shape-selective filter that is trained with prototype patterns of interest. The geometrical structure of the faces is acquired using the dual-tree complex wavelet transform (DT-CWT). Dense SIFT descriptor extracts the shape attributes of an image by building local histograms of gradient orientation. Finally, least square support vector machine (LS-SVM) is utilized to recognize the gender of an individual. The experiment was performed on self-built facial makeup for male and female (FMMF) database and achieves 89.7% accuracy.

Corresponding Author:

Annie Micheal
Department of Computer Science and Engineering, Sathyabama Institute of Science and Technology
Chennai, India
Email: annymick@gmail.com

1. INTRODUCTION

Gender recognition is getting expanding consideration since gender conveys rich and distinguished information concerning female and male. Recognizing the gender of a person without facial makeup is a challenging task. It has a few modern applications, for instance, human-computer interaction, control in smart buildings, biometrics, gender advertising, criminology, security investigation, content-based indexing, and searching. The appearance of the face can change due to the application of makeup and such a change makes gender identification a difficult task. The shape of the face is not changed much by the application of facial makeup. COSFIRE filter is a trainable shape detector. In the traditional COSFIRE filter [1], the prototype image is convolved with a bank of Gabor filters of different scales and orientations during the automatic configuration process. Nevertheless, there are two disadvantages in Gabor filter. The bandwidth cannot exceed typically one octave and Gabor filter are not optimal for covering broad spectral information with maximal spatial localization. Log-Gabor filter [2] overcomes the downsides of Gabor filter which improves the performance with its wider spectrum information and maximum spatial localization. The over-representation of low frequencies is also reduced by Log-Gabor filter. Log-Gabor filter acts as an impressive tool to extract edge information available in the high-frequency sub-components. hence Log-Gabor COSFIRE (LG-COSFIRE) filter is proposed to overcome the drawback of COSFIRE filter. A face descriptor is formed using a LG-COSFIRE filter and the differences in the shape of the female and male are captured by automatically configuring numerous LG-COSFIRE filters that are selective for different parts of the faces. Then, dual-tree complex wavelet transforms (DT-CWT) [3] is utilized to extract the geometrical structure of a face. The dense SIFT descriptor [4] extracts the local details at every pixel of an image by creating a histogram of gradient orientations and magnitudes. Finally, all three features are fused and given as input to the least square support vector machine (LS-SVM) to recognize the gender of the person. The major contributions of our work are the following

– To the best of our knowledge, this is the first work to recognize the gender of a person with facial makeup.
– A novel approach called Log-Gabor COSFIRE is proposed in our work.
– DT-CWT is chosen as a feature extraction technique for recognizing gender.
– We also contribute a new dataset of makeup faces for gender recognition.
– The performance of the system was assessed utilizing two classifiers, specifically, SVM, and LS-SVM.

We observed that LS-SVM accomplishes a better accuracy rate than SVM.

2. RELATED WORK

Rai and Khanna [5] classified gender by extracting the key features from the face using wavelet and random transform. K-nearest neighbor (KKN) [6] classifier was utilized to classify the gender into male and female. The obtained results were compared with the discrete cosine transform (DCT) [7]. The accuracy achieved for DCT was 77 % and 90 % for wavelet and random transform. Lian and Lu [8] recognized the gender under various pose by representing the facial pictures using both texture and shape information. The local binary pattern (LBP) [9] is extracted from the partitioned facial image and is given as an input to the SVM to classify the gender. Moghaddam and Yang [10] built up an appearance-based approach and nonlinear SVMs to recognize the gender. Scalzo *et al.* [11] proposed feature fusion hierarchical (FFH) with two levels. In the first level, Laplace and Gabor features are extracted from the facial image, and the extracted features are fed to feature fusion level. The fused feature is given as an input to the classifier in the second level. Genetic algorithm was used to recognize gender. Linear discriminant analysis (LDA) [12] and independent component analysis (ICA) [13] was used to identify an individual's gender [14]. A method for gender recognition from unconstrained face images was presented by Annie and Geetha [15] using kernel-based SVM and descriptions of the form and texture of the face. For classification, the method uses a SVM in conjunction with the dominant rotated LBP (DRLBP) [16], rotation invariant local phase quantization (RILPQ) [17] texture descriptor, and pyramid histogram of oriented gradient (PHOG) [18] shape descriptor. Radial basis function (RBF) kernel SVM had achieved an optimal performance of 98.7, 95.3, and 96%. Our research is the first attempt to develop a system or methodology specifically designed to recognize the gender of individuals without makeup. There hasn't been any published research or study addressing this specific problem domain. This highlights the novelty of our research in the field of gender recognition without makeup.

3. THE PROPOSED FRAMEWORK

The architecture of the proposed gender classification with facial makeup is shown in Figure 1. The proposed gender classification framework involves four steps, specifically, image acquisition, preprocessing, feature extraction and gender classification. A self-built facial makeup for male and female (FMMF) database which consist of actress and actor images is used to recognize the gender.

3.1. Preprocessing

The face is detected using a mixture of trees [19] with which, the individual look of the features, relationships among the features, and the aspect (which features are present and which features are not present) can be modeled. Modified k-means algorithm is utilized to cluster the image patches in the training images and it learns the appearances and the warped positions of the cluster centers. The similarity between the cluster center and a patch is computed based on the distance between the pixel representations with Euclidean distance. Clustering the image patches convert it to assembly, which is further used to learn the face model. After detecting the face, the image is cropped into 128×128 size. Next, we convert the RGB image into the grayscale image and apply histogram equalization technique to enhance the contrast of the image. The illumination effect is normalized by histogram equalization. Figure 2 shows the preprocessing of a sample image from the database. Figures 2(a) sample image, 2(b) the output of the face detection process, 2(c) resized image, 2(d) conversion to grayscale image, and 2(e) histogram equalization.

3.2. Feature extraction

3.2.1. LG-COSFIRE

LG-COSFIRE is a trainable shape-selective filter. We briefly explain the process to configure and apply LG-COSFIRE filter. Consequently, use their responses to form a face descriptor.

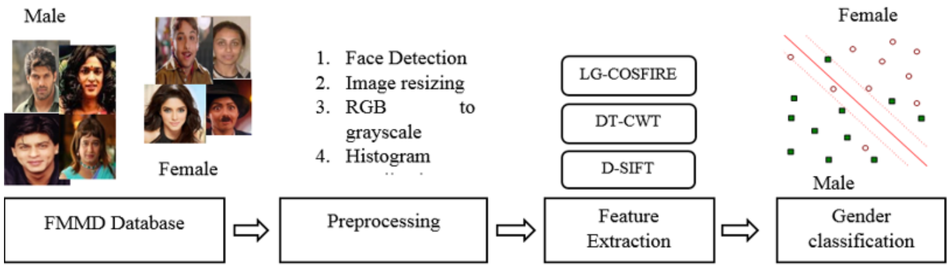

Figure 1. The proposed architecture diagram for gender classification with facial makeup

(a) (b) (c) (d) (e)

Figure 2. Preprocessing of a sample image; (a) sample image, (b) face detection, (c) image resizing, (d) grayscale conversion, and (e) histogram equalization

The LG-COSFIRE filter is configured automatically to determine the shape selectivity of a prototype pattern of interest. The prototype image is convolved with a bank of Log-Gabor filters of different scales and orientations and superimposes the resulting feature maps. Then, around the point of interest, a number of concentric circles with radii *p* are considered and the positions along these circles which attain the local maxima Log-Gabor responses are chosen. Each point *i* is expressed with four parameters $(\lambda, \theta, \rho, \varphi)$; where λ and θ represent the scale and orientation of the Log-Gabor filter that attains the maximum response at that position with distance ρ and polar angle φ with regards to the prototype center. Hence, a LG-COSFIRE filter is denoted as a set 4-tuples

$$S_f = \{(\lambda_i, \theta_i, \rho_i, \varphi_i) | i \in 1, \ldots, n\} \quad (1)$$

where *f* represents the given prototype pattern and *n* denotes the no of points that attain the local maximum Log-Gabor response. Figure 3 shows the configuration of LG-COSFIRE filter with the prototype pattern of interest selected from the training images (Figure 3(a)-3(d)). For each tuple, a pipeline of four operations is applied to compute the LG-COSFIRE filter response. First, Log-Gabor filter with scale λ_i and orientation θ_i is applied for each tuple *i* in S_f. Secondly, for the i^{th} tuple, max blurring function is applied to the corresponding Log-Gabor response map to permit tolerance in the respective position. In the blurring operation, a sliding window approach is used on the Log-Gabor response maps. In every window, the Log-Gabor responses are weighted with a Gaussian function. The standard deviation σ_i of the Gaussian function grows linearly with the distance ρ_i: $\sigma_i = \sigma_o + \alpha\rho_i$ where σ_0 and α are constant determined empirically. The weighted maximum has resulted as the output of the blurring operation. Thirdly, every blurred Log-Gabor response is moved by the polar vector $(\rho_i, -\varphi_i)$, with the goal that all the concerned Log-Gabor responses meet at the support center of the concerned LG-COSFIRE filter. Lastly, all the blurred and shifted Log-Gabor filter responses are combined by geometric mean. Therefore, LG-COSFIRE filter response r_{S_f} is denoted as:

$$r_{S_f}(x, y) = \left(\prod_{n}^{i=1} S_{\lambda_i, \sigma_i, \rho_i, \varphi_i}(x, y)\right)^{\frac{1}{n}} \quad (2)$$

A descriptor for face images is formed by utilizing the maximum responses of all LG-COSFIRE filters that are selective for different parts of female and male faces.

3.2.2. The DT-CWT

DT-CWT encompasses two trees of real filter in parallel (i.e.) Tree *a* and Tree *b*. Each of the trees comprises of a set of filters: low-pass filter (h_0&g_0) and high-pass filter (h_1&g_1). Tree *a* yield the real part and

Tree b yield the imaginary part of the complex coefficients. The DT-CWT of an input image $f(\vec{x})$ is defined by:

$$f(\vec{x}) = \sum_k W_\varphi(j_o,k)\varphi_{j_o,k}(\vec{x}) + \sum_i \sum_{j>j_o} \sum_k W_\Psi(j,k)\Psi^i_{j,k}(\vec{x}) \quad (3)$$

where $i = \pm 15^o, \pm 45^o, \pm 75^o$, $\varphi_{j_o,k}$ is the scaling function and $\Psi^i_{j,k}$ is the wavelet function (scaling function and wavelet function are complex). $W_\varphi(j_o,k)$ denotes the scaling coefficients and $W_\Psi\ (j,k)$ represents the wavelets coefficient of the transform. The transform can differentiate positive and negative frequencies and produce six sub-bands oriented in ±15, ±45, ±75. The real, imaginary, and magnitude part of DT-CWT are shown in Figure 4. The DT-CWT output as show in Figure 4(a)-4(c).

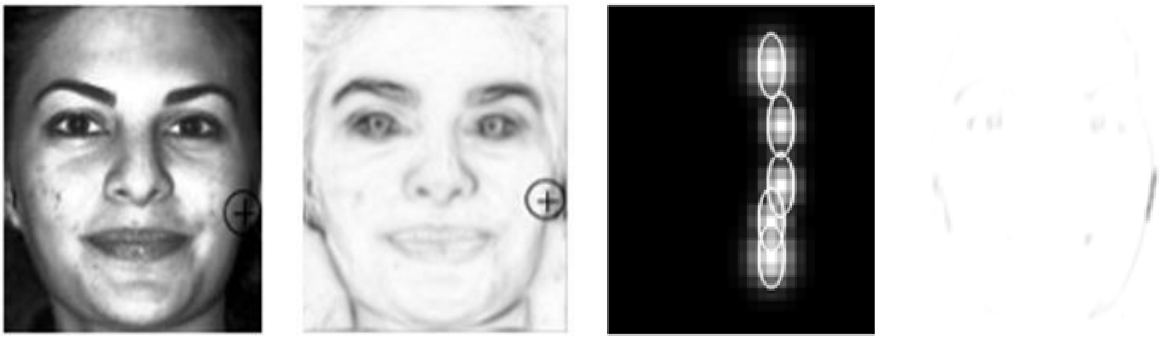

(a) (b) (c) (d)

Figure 3. Configuration of LG-COSFIRE filter; (a) training face image and the randomly selected pattern of interest, (b) the superposition (inverted) response maps of a bank of Log-Gabor filters, (c) the structure of the LG-COSFIRE filter that is selective for the encircled pattern shown in (a), and (d) the (inverted) response map of the concerned LG-COSFIRE filter to the input image in (a)

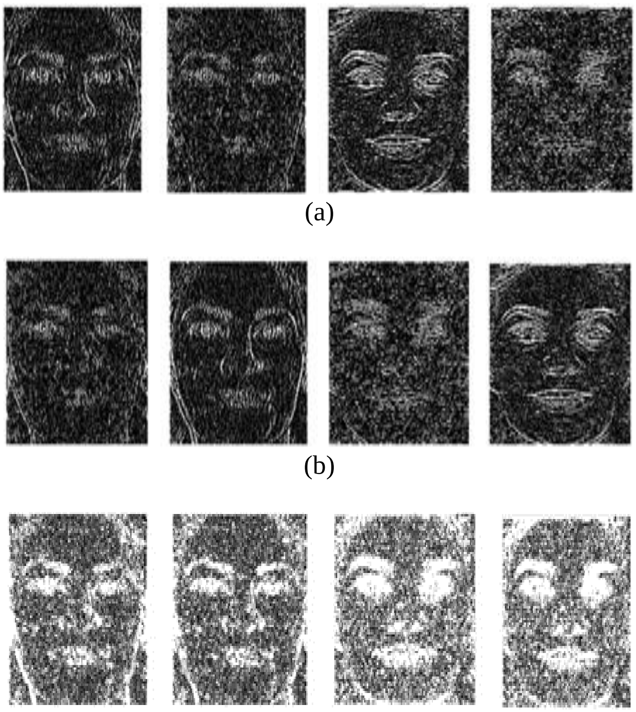

(a)

(b)

(c)

Figure 4. DT-CWT output; (a) the real part of DT-CWT for the sample image, (b) the imaginary part of DT-CWT for the sample image, and (c) the magnitude part of DT-CWT for the sample image

3.2.3. Dense SIFT

In dense SIFT descriptor, a local feature descriptor can be extracted for every pixel in an image. First, the local region around the pixel is divided into number of cells. Then, the gradient information in every cell is characterized by employing an orientation histogram with numerous bins. For every cell, its histogram is built by gathering the gradient magnitude of all the pixels in a cell into a corresponding bin that is selected according to the gradient orientation of the pixel. Thus, a feature descriptor is created for every pixel. Figure 5 shows the visualization of the dense SIFT feature. SIFT output as show in Figure 5(a)-5(b).

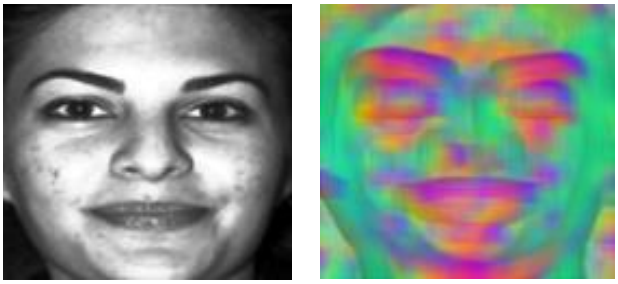

(a) (b)

Figure 5. Dense SIFT output (a) sample image and (b) dense SIFT feature visualization for the sample image

3.3. LS-SVM

LS-SVM was proposed by Suykens and Vandewalle [20]. The difference between SVM and LS-SVM is that LS-SVM uses a set of linear equations instead of a quadratic equation as in classical SVM. The formulation of LS-SVM includes equality type constraints.

$$\min_{\omega,b,l} J(\omega,b,l) = \frac{1}{2}\omega^T\omega + \gamma\frac{1}{2}\sum_{i=1}^{n} l_i^2 \tag{4}$$

Subject to equality constraint:

$$y_i[\omega^T\phi(x_i) + b] - 1 + l_i, i = 1,2,\dots,N \tag{5}$$

where $\phi(.)$ is the mapping function which maps input space into higher dimensional space, ω is the weight vector, l is the error, and γ is the regularization factor. The Lagrangian is written as:

$$L(\omega,b,l;\alpha) = J(\omega,b,l) - \sum_{i=1}^{N}\alpha_i y_i[\omega^T\phi(x_i) + b] - 1 + l_i \tag{6}$$

the LS-SVM classifier function is defined as,

$$f(x) = sign[\sum_{i=1}^{N}\alpha_i y_i k(x,x_i) + b] \tag{7}$$

where, $k(x,x_i) = exp(-\gamma\|x - x_i\|^2)$ is the RBF kernel.

4. EXPERIMENTAL DETAILS AND RESULT ANALYSIS

4.1. Dataset description

FMMF database has been generated which consists of actress and actor images since existing makeup datasets like facial cosmetic database (FCD) [21], YouTube makeup database (YMU) [22], makeup in the wild (MIW) [23], virtual makeup dataset (VMU), and makeup induced face spoofing (MIFS) [24] contains only female images. The generated database consists of 3,840 images (2,106 female and 1,734 male) with 640 subjects. The proposed methodology is implemented in MATLAB 2015b version. Sample images from the database are shown in Figure 6. 6 images for each individual where 3 images are without facial makeup in Figure 6(a) and 3 images with facial makeup in Figure 6(b).

(a) (b)

Figure 6. Images from the FMMD database (a) images without makeup and (b) images with makeup

4.2. Preprocessing

The face is detected from the sample images. The facial region is resized to 128*128 pixels and converted to a grayscale image. After that, histogram equalization technique is performed to assign an equal number of pixels to all gray levels.

4.3. LG-COSFIRE filter

We configured 180 LG-COSFIRE filters for the FMMF datasets. For each randomly chosen image, a region of 19*19 pixel is chosen and used it as a prototype pattern to configure a LG-COSFIRE filter. The selected prototype is considered as a valid prototype if its corresponding LG-COSFIRE is with at least five tuples. Otherwise, we reject the prototype and chose another prototype. We performed different k-fold cross validation such as 3-fold, 5-fold, and 10-fold cross-validation using SVM and LS-SVM to compute the accuracy of the proposed system. Table 1 shows the results of LG-COSFIRE filter compared with the traditional COSFIRE for different k-fold cross-validation using SVM and LS-SVM classifiers with RBF kernel. Accuracy (ACC) is defined as the percentage of images classified correctly to the total no of images. Male classification (MC) and female classification (FC) is the percentage of male and female images classified correctly to the total no of male and female images. The best outcome is marked in bold.

4.4. DT-CWT

The DT-CWT descriptor is extracted at different levels (L=1,2,3,4). Tables 2 show the accuracy rate for 3-fold, 5-fold, and 10-fold cross-validation at different levels using SVM and LS-SVM. Male classification rate and female classification rate are also calculated for DT-CWT at different levels using SVM and LS-SVM. 83.1% and 64.2% is the highest male and female classification rate obtained for LS-SVM with 10-fold cross-validation at level 4. From the experimental results, it was observed that the accuracy rate is higher at level 4 for LS-SVM with 3-fold, 5-fold, and 10-fold cross-validation.

Table 1. Results for LG-COSFIRE filter using SVM and LS-SVM for different k-fold cross-validation

Method	K-fold CV	SVM			LS-SVM		
		FC (%)	MC (%)	ACC (%)	FC (%)	MC (%)	ACC (%)
COSFIRE	3-fold	50.1	65.1	59.3	52.1	66.3	61.9
	5-fold	51.7	65.8	59.8	53.8	67.8	62.5
	10-fold	52.2	66.3	60.4	54.6	68.9	62.8
LG-COSFIRE	3-fold	65.9	84.9	76.8	68.2	87.2	79.1
	5-fold	66.4	85.4	77.1	68.7	88.3	79.8
	10-fold	67.2	86.1	77.9	69.3	88.9	80.3

Table 2. Result for DT-CWT at different level using SVM and LS-SVM with different k-fold cross-validation

Method	K-fold CV	Parameter Level	SVM			LS-SVM		
			FC (%)	MC (%)	ACC (%)	FC (%)	MC (%)	ACC (%)
DTCWT	3-fold	1	52.5	69.7	63.2	58.9	78.8	73.6
		2	53.1	69.1	63.5	58.5	78.6	73.1
		3	52.8	69.6	63.1	59.2	78.3	73.8
		4	52.6	69.9	63.5	59.6	79.1	74.2
	5-fold	1	55.0	71.6	64.8	61.8	80.2	75.2
		2	55.6	71.2	65.1	61.2	81.0	75.6
		3	55.2	72.2	65.2	61.7	80.6	75.1
		4	56.5	72.5	65.9	62.2	81.7	75.8
	10-fold	1	57.3	73.5	66.2	63.2	82.8	78.2
		2	56.1	73.2	67.7	63.9	82.4	77.5
		3	57.5	74.6	67.5	63.3	82.7	77.9
		4	57.8	74.8	67.9	64.2	83.1	78.7

4.5. Dense SIFT

For extracting dense SIFT feature, a publicly available toolbox [25] was utilized. A descriptor is created by applying a 4×4 cell array and an 8-bin orientation histogram in every cell. The size of the neighborhood (i.e., scale factor) is important for extracting the D-SIFT descriptor. Therefore, the performance of the system was analyzed for different scale factors such as 8×8, 16×16, 24×24, 32×32, 40×40, and 48×48. Table 3 show the classification results for 3-fold, 5-fold, and 10-fold cross-validation with different scale factors using SVM and LS-SVM classifier. The accuracy classification is better for scale factor 24×24 using LS-SVM with 3-fold, 5-fold, and 10-fold cross-validation. It is proven from the experimental outcomes that 10-fold cross-validation provides better accuracy than 3-fold and 5-fold cross-validation. Hence, further analysis was conducted using 10-fold cross-validation only. The best attribute of every approach, which provides the best accuracy is fixed. Table 4 shows the results of two feature combinations. The proposed LG-COSFIRE is combined with D-SIFT, and DTCWT which yields a higher classification rate of 89.7% for images without makeup see in Table 5.

Table 3. Result for D-SIFT for different scale factor using SVM and LS-SVM with different k-fold cross-validation

Method	K-fold CV	Parameter	SVM			LS-SVM		
		Scale factor (SF)	FC (%)	MC (%)	ACC (%)	FC (%)	MC (%)	ACC (%)
D-SIFT		8×8	40.6	53.3	49.5	42.6	56.7	51.4
	3-fold	16×16	46.3	61.1	55.6	48.7	63.4	58.6
		24×24	48.7	63.2	56.4	51.8	65.8	61.9
		32×32	45.4	58.2	54.3	47.2	59.4	56.3
		40×40	43.5	56.1	53.6	46.3	58.8	55.7
		48×48	42.2	55.7	51.9	44.7	57.3	52.6
		8×8	42.1	54.7	51.5	44.8	59.3	52.3
		16×16	47.5	61.5	57.0	50.2	64.0	59.2
	5-fold	24×24	49.6	64.3	59.9	52.1	66.3	62.5
		32×32	46.1	62.6	55.2	48.4	63.2	57.6
		40×40	44.7	58.7	54.5	47.2	62.1	56.3
		48×48	42.9	56.5	52.4	45.8	61.8	53.5
		8×8	42.5	56.6	53.8	45.3	61.9	54.7
		16×16	49.1	62.7	59.4	52.9	66.4	61.5
		24×24	50.8	65.4	61.5	55.6	67.9	63.8
	10-fold	32×32	47.4	63.2	58.6	50.7	64.5	59.6
		40×40	45.8	61.3	56.2	48.9	63.7	57.4
		48×48	43.6	59.5	54.8	46.2	62.2	55.9

Table 4. Result for two feature analysis using SVM and LS-SVM with 10-fold cross-validation

Method	Parameter	SVM			LS-SVM		
		FC (%)	MC (%)	ACC (%)	FC (%)	MC (%)	ACC (%)
LG-COSFIRE+D-SIFT	SF=24×24	68.9	84.8	79.5	73.9	88.7	83.8
DT-CWT+DSFIT	L=4, SF=24×24	66.8	81.5	75.6	71.7	86.3	80.5
LG-COSFIRE+DT-CWT	L=4	70.1	85.7	82.1	75.2	90.9	85.8

Table 5. Result for three feature analysis using SVM and LS-SVM with 10-fold cross-validation

Method	Parameter	SVM			LS-SVM		
		FC (%)	MC (%)	ACC (%)	FC (%)	MC (%)	ACC (%)
LG-COSFIRE+D-SIFT+DT-CWT	SF=24×24, L=4	78.3	90.5	85.3	81.4	94.3	89.7

5. CONCLUSION

This study investigated the effects of recognizing the gender of an individual with facial makeup. This is the first work to recognize the gender of a person with facial makeup. The research proposes a novel approach called Log-Gabor COSFIRE. The differences in the shape of the female and male are captured by automatically configuring numerous LG-COSFIRE filters that are selective for different parts of the face. The geometrical structure of an image is estimated using DT-CWT. The shape attributes of an image were extracted utilizing dense SIFT descriptor by building local histograms of gradient orientation. SVM and LS-SVM classifiers are trained using k-fold cross-validation. The performance of the proposed approach was evaluated using a self-built FMMD database. When LG-COSFIRE is combined with DT-CWT and D-SIFT, 89.7% classification accuracy is obtained using LS-SVM with 10-fold cross-validation. Hence the proposed LG-COSFIRE feature contributes a high accuracy rate for gender recognition with facial makeup.

There hasn't been any known research or study that specifically focused on recognizing gender from facial images where the individuals are wearing makeup. This highlights the novelty and uniqueness of our research. The research also contributes a new dataset consisting of images of faces with makeup. Recognizing the gender of a person with makeup is important in applications such as human computer interaction, biometrics, content-based indexing and searching. Gender recognition with facial makeup can prevent men to defraud women. In the future, the gender of a person can be recognized with facial images with heavy makeup.

REFERENCES

[1] G. Azzopardi and N. Azzopardi, "Trainable COSFIRE filters for keypoint detection and pattern recognition," *IEEE Transactions on Pattern Analysis and Machine Intelligence*, vol. 35, no. 2, pp. 490–503, Feb. 2013, doi: 10.1109/TPAMI.2012.106.

[2] D. J. Field, "Relations between the statistics of natural images and the response properties of cortical cells," *Journal of the Optical Society of America A*, vol. 4, no. 12, pp. 2379–2394, 1987.

[3] C. C. Liu and D. Q. Dai, "Face recognition using dual-tree complex wavelet features," *IEEE Transactions on Image Processing*, vol. 18, no. 11, pp. 2593–2599, 2009, doi: 10.1109/TIP.2009.2027361.

[4] C. Liu, J. Yuen, and A. Torralba, "Sift flow: dense correspondence across scenes and its applications," *Dense Image Correspondences for Computer Vision*, pp. 15–49, 2015, doi: 10.1007/978-3-319-23048-1_2.

[5] P. Rai and P. Khanna, "Gender classification using radon and wavelet transforms," *2010 5th International Conference on Industrial and Information Systems, ICIIS 2010*, pp. 448–451, 2010, doi: 10.1109/ICIINFS.2010.5578661.

[6] Y. Huan, L. Wu, L. Xu, P. Li, and T. Wei, "Superior energy-storage density and ultrahigh efficiency in KNN-based ferroelectric ceramics via high-entropy design," *Journal of Materiomics*, Apr. 2024, doi: 10.1016/j.jmat.2024.03.007.

[7] S. P. Bharadwaj, "A discrete cosine transform-based rapid algorithm for high-resolution, full-spectrum calculations over inhomogeneous gas paths," *Journal of Quantitative Spectroscopy and Radiative Transfer*, vol. 316, p. 108895, Apr. 2024, doi: 10.1016/j.jqsrt.2024.108895.

[8] H. C. Lian and B. L. Lu, "Multi-view gender classification using local binary patterns and support vector machines," *Lecture Notes in Computer Science (including subseries Lecture Notes in Artificial Intelligence and Lecture Notes in Bioinformatics)*, vol. 3972 LNCS, pp. 202–209, 2006, doi: 10.1007/11760023_30.

[9] C. Ozdemir, Y. Dogan, and Y. Kaya, "A new local pooling approach for convolutional neural network: local binary pattern," *Multimedia Tools and Applications*, vol. 83, no. 12, pp. 34137–34151, 2024, doi: 10.1007/s11042-023-17540-x.

[10] B. Moghaddam and M.-H. Yang, "Learning gender with support faces," *IEEE Transactions on Pattern Analysis and Machine Intelligence*, vol. 24, no. 5, pp. 707–711, May 2002, doi: 10.1109/34.1000244.

[11] F. Scalzo, G. Bebis, M. Nicolescu, L. Loss, and A. Tavakkoli, "Feature fusion hierarchies for gender classification," in *Proceedings - International Conference on Pattern Recognition*, IEEE, Dec. 2008, pp. 1–4. doi: 10.1109/icpr.2008.4761234.

[12] R. Graf, M. Zeldovich, and S. Friedrich, "Comparing linear discriminant analysis and supervised learning algorithms for binary classification a method comparison study," *Biometrical Journal*, vol. 66, no. 1, 2024, doi: 10.1002/bimj.202200098.

[13] A. Hameed *et al.*, "Temporal–spatial transformer based motor imagery classification for BCI using independent component analysis," *Biomedical Signal Processing and Control*, vol. 87, 2024, doi: 10.1016/j.bspc.2023.105359.

[14] A. Jain and J. Huang, "Integrating independent components and linear discriminant analysis for gender classification," *Proceedings - Sixth IEEE International Conference on Automatic Face and Gesture Recognition*, pp. 159–163, 2004, doi: 10.1109/AFGR.2004.1301524.

[15] A. A. Micheal and P. Geetha, "Combined feature extraction for multi-view gender recognition," *Smart Innovation, Systems and Technologies*, vol. 104, pp. 219–228, 2019, doi: 10.1007/978-981-13-1921-1_22.

[16] R. Mehta and K. Egiazarian, "Dominant rotated local binary patterns (DRLBP) for texture classification," *Pattern Recognition Letters*, vol. 71, pp. 16–22, 2016, doi: 10.1016/j.patrec.2015.11.019.

[17] V. Ojansivu, E. Rahtu, and J. Heikkilä, "Rotation invariant local phase quantization for blur insensitive texture analysis," *Proceedings - International Conference on Pattern Recognition*, 2008, doi: 10.1109/icpr.2008.4761377.

[18] M. A. Shirzi and M. R. Kermani, "Real-time point recognition for seedlings using kernel density estimators and pyramid histogram of oriented gradients," *Actuators*, vol. 13, no. 3, 2024, doi: 10.3390/act13030081.

[19] S. Ioffe and D. Forsyth, "Mixtures of trees for object recognition," in *Proceedings of the IEEE Computer Society Conference on Computer Vision and Pattern Recognition*, IEEE Comput. Soc, 2001, pp. II-180-II–185. doi: 10.1109/cvpr.2001.990953.

[20] J. A. K. Suykens and J. Vandewalle, "Least squares support vector machine classifiers," *Neural Processing Letters*, vol. 9, no. 3, pp. 293–300, 1999, doi: 10.1023/A:1018628609742.

[21] M. L. Eckert, N. Kose, and J. L. Dugelay, "Facial cosmetics database and impact analysis on automatic face recognition," *2013 IEEE International Workshop on Multimedia Signal Processing, MMSP 2013*, pp. 434–439, 2013, doi: 10.1109/MMSP.2013.6659328.

[22] A. Dantcheva, C. Chen, and A. Ross, "Can facial cosmetics affect the matching accuracy of face recognition systems?," *2012 IEEE 5th International Conference on Biometrics: Theory, Applications and Systems, BTAS 2012*, pp. 391–398, 2012, doi: 10.1109/BTAS.2012.6374605.

[23] C. Chen, A. Dantcheva, and A. Ross, "Automatic facial makeup detection with application in face recognition," *Proceedings - 2013 International Conference on Biometrics, ICB 2013*, 2013, doi: 10.1109/ICB.2013.6612994.

[24] C. Chen, A. Dantcheva, T. Swearingen, and A. Ross, "Spoofing faces using makeup: an investigative study," *2017 IEEE International Conference on Identity, Security and Behavior Analysis, ISBA 2017*, 2017, doi: 10.1109/ISBA.2017.7947686.

[25] A. Vedaldi, B. Fulkerson, and B. Fulerson, "VLFeat: An open and portable library of computer vision algorithms," in *Proceedings of the 18th ACM international conference on Multimedia*, New York, NY, USA: ACM, Oct. 2010, pp. 1469–1472. doi: 10.1145/1873951.1874249.

BIOGRAPHIES OF AUTHORS

Annie Micheal the author completed her Ph.D. degree in the Department of Information Science and Technology at Anna University, CEG campus, India. Currently she is working as Assistant Professor in Sathyabama Institute of Science and Technology, India. Her research interest includes image processing, computer vision, pattern recognition, and machine learning. She can be contacted at email: annymick@gmail.com.

Geetha Palanisamy the author is an Associate Professor in the Department of Information Science and Technology, College of Engineering, Anna University, Chennai, India. She completed her Doctorate and Post Graduate degree from Sathyabama University, Chennai, India. Her area of research includes machine learning, information retrieval, database management systems, data mining, and soft computing. She can be contacted at email: geethap@annauniv.edu.